Research Article | Vol. 9, No. 8 | 1 Aug 2018 | BIOMEDICAL OPTICS EXPRESS 3915
Biomedical Optics EXPRESS

Voltage-sensitive dye delivery through the blood brain barrier using adenosine receptor agonist regadenoson

Rebecca W. Pak,[1,*] Jeeun Kang,[2] Heather Valentine,[2] Leslie M. Loew,[3] Daniel L. J. Thorek,[2] Emad M. Boctor,[2] Dean F. Wong,[2] and Jin U. Kang[4]

[1]*Biomedical Engineering, Johns Hopkins University School of Medicine, Baltimore, MD, USA*
[2]*Radiology and Radiological Sciences, Johns Hopkins University School of Medicine, Baltimore, MD, USA*
[3]*R. D. Berlin Center for Cell Analysis and Modeling, University of Connecticut School of Medicine, Farmington, CT, USA*
[4]*Electrical and Computer Engineering, Johns Hopkins University Whiting School of Engineering, Baltimore, MD, USA*
**rpak2@jhmi.edu*

Abstract: Optical imaging of brain activity has mostly employed genetically manipulated mice, which cannot be translated to clinical human usage. Observation of brain activity directly is challenging due to the difficulty in delivering dyes and other agents through the blood brain barrier (BBB). Using fluorescence imaging, we have demonstrated the feasibility of delivering the near-infrared voltage-sensitive dye (VSD) IR-780 perchlorate to the brain tissue through pharmacological techniques, via an adenosine agonist (regadenoson). Comparison of VSD fluorescence of mouse brains without and with regadenoson showed significantly increased residence time of the fluorescence signal in the latter case, indicative of VSD diffusion into the brain tissue. Dose and timing of regadenoson were varied to optimize BBB permeability for VSD delivery.

© 2018 Optical Society of America under the terms of the OSA Open Access Publishing Agreement

OCIS codes: (170.2520) Fluorescence microscopy; (170.2655) Functional monitoring and imaging; (170.3880) Medical and biological imaging.

References and links

1. A. D. Mehta, J. C. Jung, B. A. Flusberg, and M. J. Schnitzer, "Fiber optic in vivo imaging in the mammalian nervous system," Curr. Opin. Neurobiol. **14**(5), 617–628 (2004).
2. C. Grienberger and A. Konnerth, "Imaging calcium in neurons," Neuron **73**(5), 862–885 (2012).
3. M. Paukert, A. Agarwal, J. Cha, V. A. Doze, J. U. Kang, and D. E. Bergles, "Norepinephrine controls astroglial responsiveness to local circuit activity," Neuron **82**(6), 1263–1270 (2014).
4. S. Chemla and F. Chavane, "Voltage-sensitive dye imaging: Technique review and models," J. Physiol. Paris **104**(1-2), 40–50 (2010).
5. E. W. Miller, J. Y. Lin, E. P. Frady, P. A. Steinbach, W. B. Kristan, Jr., and R. Y. Tsien, "Optically monitoring voltage in neurons by photo-induced electron transfer through molecular wires," Proc. Natl. Acad. Sci. U.S.A. **109**(6), 2114–2119 (2012).
6. S. I. Rapoport, "Osmotic opening of the blood-brain barrier: principles, mechanism, and therapeutic applications," Cell. Mol. Neurobiol. **20**(2), 217–230 (2000).
7. C. Saraiva, C. Praça, R. Ferreira, T. Santos, L. Ferreira, and L. Bernardino, "Nanoparticle-mediated brain drug delivery: Overcoming blood-brain barrier to treat neurodegenerative diseases," J. Control. Release **235**, 34–47 (2016).
8. G.-H. Son, B.-J. Lee, and C.-W. Cho, "Mechanisms of drug release from advanced drug formulations such as polymeric-based drug-delivery systems and lipid nanoparticles," J. Pharm. Investig. **47**(4), 287–296 (2017).
9. Q.-L. Zhou, Z.-Y. Chen, Y.-X. Wang, F. Yang, Y. Lin, and Y.-Y. Liao, "Ultrasound-mediated local drug and gene delivery using nanocarriers," BioMed Res. Int. **2014**, 963891 (2014).
10. P.-C. Chu, H.-L. Liu, H.-Y. Lai, C.-Y. Lin, H.-C. Tsai, and Y.-C. Pei, "Neuromodulation accompanying focused ultrasound-induced blood-brain barrier opening," Sci. Rep. **5**(1), 15477–15489 (2015).
11. J. J. Choi, K. Selert, F. Vlachos, A. Wong, and E. E. Konofagou, "Noninvasive and localized neuronal delivery using short ultrasonic pulses and microbubbles," Proc. Natl. Acad. Sci. U.S.A. **108**(40), 16539–16544 (2011).
12. A. J. Carman, J. H. Mills, A. Krenz, D.-G. Kim, and M. S. Bynoe, "Adenosine receptor signaling modulates

#330308 https://doi.org/10.1364/BOE.9.003915
Journal © 2018 Received 18 May 2018; revised 14 Jul 2018; accepted 23 Jul 2018; published 30 Jul 2018

Biomedical Optics EXPRESS

permeability of the blood-brain barrier," J. Neurosci. **31**(37), 13272–13280 (2011).
13. D.-G. Kim and M. S. Bynoe, "A2A adenosine receptor modulates drug efflux transporter P-glycoprotein at the blood-brain barrier," J. Clin. Invest. **126**(5), 1717–1733 (2016).
14. D.-G. Kim and M. S. Bynoe, "A2A Adenosine Receptor Regulates the Human Blood-Brain Barrier Permeability," Mol. Neurobiol. **52**(1), 664–678 (2015).
15. Y. Duan, B. Q. Yang, C. C. Chang, J. Zhou, H. Y. Li, Z. H. Xu, Z. W. Wang, and D. Y. Li, "[Preliminary study on assessment of lexiscan-induced blood-brain barrier opening and its level by CT perfusion imaging]," Zhonghua Yi Xue Za Zhi **96**(35), 2825–2829 (2016).
16. P. J. Sims, A. S. Waggoner, C.-H. Wang, and J. F. Hoffman, "Studies on the Mechanism by Which Cyanine Dyes Measure Membrane Potential in Red Blood Cells and Phosphatidylcholine Vesicles," Biochemistry **13**(16), 3315–3330 (1974).
17. M. Reers, T. W. Smith, and L. B. Chen, "J-aggregate formation of a carbocyanine as a quantitative fluorescent indicator of membrane potential," Biochemistry **30**(18), 4480–4486 (1991).
18. A. S. Waggoner, "Dye Indicators of Membrane Potential," Annu. Rev. Biophys. Bioeng. **8**(1), 47–68 (1979).
19. J. S. Treger, "Sensors and probes: A universal voltage indicator," Nat. Methods **11**(107), L09–L12 (2014).
20. J. S. Treger, M. F. Priest, R. Iezzi, and F. Bezanilla, "Indocyanine Green is a Voltage-Sensitive Fluorescent Dye," Biophys. J. **106**(2), 793a (2014).
21. H. K. Zhang, P. Yan, J. Kang, D. S. Abou, H. N. D. Le, A. K. Jha, D. L. J. Thorek, J. U. Kang, A. Rahmim, D. F. Wong, E. M. Boctor, and L. M. Loew, "Listening to membrane potential: photoacoustic voltage-sensitive dye recording," J. Biomed. Opt. **22**(4), 045006 (2017).

Introduction

It is established that cellular activity in the brain forms the basis for animal behavior. Yet the complexity of neuronal architecture and the privileged anatomical location of the brain represent long standing impediments to understanding the brain and how best to treat neurological disorders. Current non-invasive techniques rely on bulk effects and thus, do not give cellular resolution. There have been a number of optical imaging approaches to directly monitor brain activity with high spatial and temporal resolution. These include one-photon fluorescence microendoscopy, two-photon confocal microscopy, and endoscopic fiber imaging [1–3]. To visualize brain activity without genetic manipulation, functional fluorescent dyes have been employed, with one of the most widely used types being voltage-sensitive dyes (VSDs) [4]. While VSDs enable individual neuron monitoring with fast time responses and have the ability to operate without modification of the subject, drawbacks include potential toxicity and lower signal-to-noise ratio compared to genetically encoded indicators [5]. Many common VSDs also operate within the visible wavelength range, leading to shallow imaging depth due to absorption. Another challenging aspect of using VSDs is the delivery of dye to the brain.

A variety of methods have been investigated for drug and dye delivery through the blood brain barrier (BBB), a highly-selective semipermeable membrane separating the blood from the brain tissue and extracellular fluid. Osmotic opening of the BBB in which a solution of arabinose or mannitol is infused into the brain has been used for therapeutic applications, but is invasive and causes transient brain edema and gradual dehydration that likely affect neurological activity [6]. Nanocages and nanoparticles have also been considered, but pose the risk of potential toxicity due to their persistence in the body [7]. Additionally, many factors influence the release of contents from nanocages and the mechanisms depend on diffusion, osmosis, and degradation that must be tuned [8]. Without proper delivery of the VSD to the brain tissue, there would be no VSD fluorescence reporting neural activity. Focused-ultrasound (FUS) was considered as well, but often requires incorporation of the drugs into nanoparticles or microbubbles [9]. There is also some evidence that FUS is accompanied by neuromodulation [10] and since it creates mechanical stress on the cell junctions, risks include hemorrhage and neuron damage [11]. Alternatively, studies have shown that activation of adenosine receptors increases BBB permeability [12–15]. Thus, to address the delivery obstacle while also facilitating deeper brain imaging, we evaluated the effectiveness as well as the optimal timing and dose of the FDA-approved adenosine receptor agonist regadenoson (tradename Lexiscan) injected with near-infrared (NIR) VSD IR-780. With the increased BBB permeability due to regadenoson, the VSD was able to diffuse into

Biomedical Optics EXPRESS

the brain tissue, facilitating the monitoring of neuronal cell activity minimally invasively through the intact skull.

Methods

In this study, IR-780 perchlorate, an NIR cyanine VSD was used to study the effectiveness of regadenoson. The use of an NIR VSD increased imaging depth and provided the opportunity to image the brain through the intact skull. Due to the delocalized positive charge of the dye, hyperpolarization led to uptake of the dye into the neurons, whereas depolarization resulted in dye leaving the cells [16]. Cyanine dye molecules (i.e. the commonly used indocyanine green and variants such as IR-780 perchlorate) have a history of being used for voltage sensing [16–20] since they form non-fluorescent aggregates when in high concentrations, thus leading to quenched fluorescence at the resting membrane potential [21]. On the other hand, action potential firing releases the dye into the extracellular space to cause an increase in the fluorescence signal. Thus, fluorescence imaging of VSDs provides an effective method for monitoring neuron activity. However, VSDs must be delivered to the brain, which can be challenging due to the brain's immune privilege and BBB.

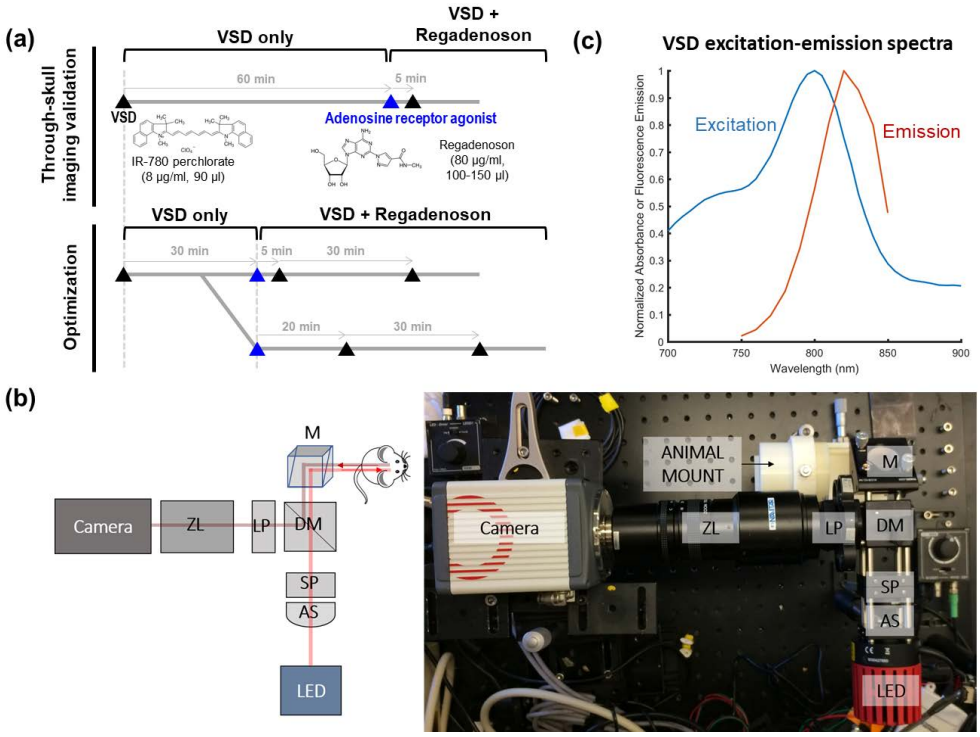

Fig. 1. (a) *In vivo* experimental protocol, (b) NIR fluorescence system setup: AS = aspheric lens, SP = shortpass filter, M = mirror, DM = dichroic mirror, LP = longpass filter, ZL = zoom lens, and (c) VSD spectral characteristics.

To test the effects of regadenoson (Astellas Pharma US, Inc.) on IR-780 perchlorate (576409, Sigma-Aldrich Corp., OS) VSD diffusion, 35-50 g CD1 mice (Charles Rivers Laboratory, Inc., MA, N = 7) were anesthetized with a 50:1 solution of ketamine:xylazine. 24G x ¾" intravenous (iv) tail vein catheters (Terumo Corporation) were placed for injection consistency. To demonstrate the potential for non-invasive procedures, only the scalp skin was removed for the first 3 mice. These mice received iv tail vein injections according to the *through-skull imaging validation* protocol in Fig. 1(a).

Biomedical Optics EXPRESS

To verify and quantify dye diffusion, a craniotomy was performed on each of the remaining mice so scattering from the skull could be distinguished from diffusion into the tissue. A head fixation mount was fastened to the skull using dental cement. A dental drill was used to create a 6 x 7 mm^2 cranial window. The skull piece was removed and replaced by a #1 thick (130-160 μm) glass coverslip cut to size, also secured using dental cement. After recovering from the craniotomy procedures for at least a week, the mice received tail vein injections in a similar schedule as before. However, the monitoring time for each injection was shortened since the first study with intact skulls showed the fluorescence intensity reaching a steady state around 15-20 min after VSD injection. The craniotomy study injections followed the *optimization protocol* in Fig. 1(a).

NIR fluorescence imaging was used to assess dye diffusion, particularly to evaluate optimal injection time and dose of regadenoson for best dye diffusion into the brain tissue. A typical fluorescence imaging setup (Fig. 1(b)) was employed with an 800 mW LED light source, operating at a center wavelength of 780 nm and an achromatic lens as a condenser. A dichroic mirror at 805 nm separated the excitation and emission light. Additional filtration was accomplished with excitation and emission filters. This high-sensitivity imaging system enables sensing of VSD fluorescence with excitation-emission spectral characteristics shown in Fig. 1(c). Focusing and magnification was achieved with a zoom lens (Navitar Inc.) attached to an sCMOS camera (Hamamatsu Photonics). For the *optimization* craniotomy study, mice were head-fixed to avoid motion artifacts from breathing.

To account for differences in injection timing, the time sequences of the VSD only and VSD + regadenoson conditions were synchronized by aligning *injection peaks* (the maximum of the fluorescence signals, indicated in Fig. 3 center panel). Before each dye injection, a background image was taken. After the experiment, the corresponding background image was subtracted from each 30 min sequence of images to examine fluorescence contributions due only to that particular dye injection and reject any fluorescence signal remaining from previous injections or autofluorescence. In order to compare the VSD only condition to the VSD + regadenoson condition, the *condition subtraction* curve, a differential fluorescence intensity trace between VSD and VSD + regadenoson conditions (indicated in Fig. 3 center panel), was calculated pixel-by-pixel. Regions of interest (ROIs) were chosen to reflect large in-focus vasculature versus microvasculatures. Average VSD fluorescence intensity over the ROIs was plotted.

A histological verification study was conducted using three Sprague Dawley rats weighing 280-350 g. The first rat was injected with regadenoson alone, the second one was injected with regadenoson followed 5 min later by IR-780 VSD, and the third was injected with IR-780 VSD only. All rats were sacrificed 1-hour post injection(s). The whole brains of the rats were immediately harvested and placed in fresh 10% formalin for > 48 hours with gentle agitation using a conical rotator. Cryoprotection processing was done via a series of sucrose gradients (15%, 20%, 30% for 12-24 hours each). Brains were frozen-sectioned at 300 μm thickness. Slides with tissue sections in ProLong Diamond Anti-face mountant were imaged using the LI-COR Odyssey for fluorescence visualization of VSD perfusion.

Results

Through-skull fluorescence imaging validated the capability of the system and VSD to be used minimally-invasively. In this first study in which only the scalp was removed and the skull remained intact, the fluorescence signal decay was compared between the VSD only and VSD + regadenoson conditions. An exponential curve was fit following the model $\alpha + \beta e^{-\frac{t}{\tau}}$ for which the exponential decay coefficient, γ, was defined as $\gamma = 1/\tau$. As shown in Fig. 2(a) where the y-axis represents the normalized mean fluorescence signal over the whole mouse brain after normalization, a much faster decay in fluorescence signal was observed without regadenoson. The faster decay of the fluorescence normalized mean intensity without

Biomedical Optics EXPRESS

regadenoson implies that after the initial peak in fluorescence due to the systemic VSD injection, the VSD remains mostly within the circulation and vessels then decays as the body gets rid of the dye as waste. It should be noted that since IR-780 perchlorate is a small molecule VSD, it is capable of some natural diffusion through the vessels and permeation into the brain tissue as shown by the long background signal. The longer mean time constant when regadenoson was injected ($\overline{\tau_{Regad}} = 3.4$ min compared to $\overline{\tau_{WithoutRegad}} = 1.9$ min) suggests that a larger percentage of VSD is penetrating into the brain tissue through the BBB with regadenoson. Hence, the fluorescence signal remained stronger for longer since the dye in the brain tissue exhibited a longer diffusion time of tens of minutes. Thus, the slowed VSD fluorescence decay with regadenoson suggests a greater BBB penetration. The difference in exponential decay coefficients was compared by the t-test and statistical significance was validated: p = 0.0146. Additionally, this trend can be visually observed in the background subtracted images from each condition at 5-min intervals (Fig. 2(b)).

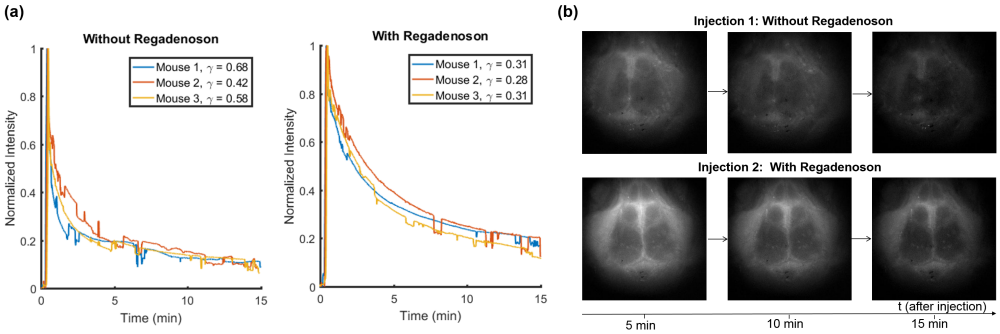

Fig. 2. Through-skull (a) decay curves and (b) image time sequence showing fluorescence signal without and with regadenoson.

Optimization of the dosage and timing of regadenoson administration was also conducted to achieve optimal VSD diffusion into the brain tissue. After processing and aligning images as outlined in the Methods, the mean fluorescence intensity for *condition subtraction* curves for chosen ROIs corresponding to large vessels (red and yellow curves), brain tissue and microvasculatures (green and blue), and background (black) were plotted (Fig. 3). The *injection* curves (dashed blue and magenta curves for VSD only and VSD + regadenoson, respectively) were also plotted to observe the timing, but were scaled for better visualization. A time delay can be observed between the *injection peaks* and the increase in the *condition subtraction* curves.

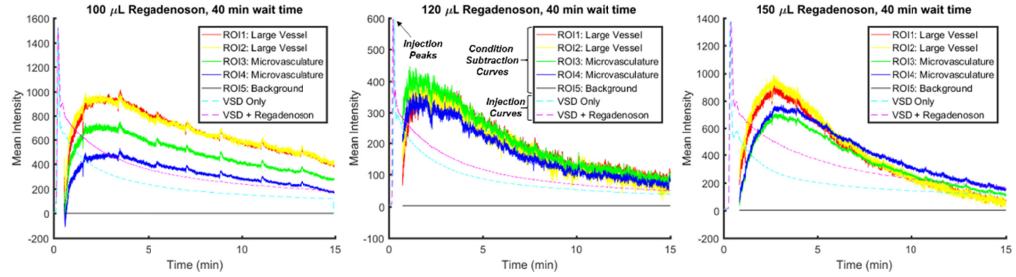

Fig. 3. Sample scaled *injection* curves (dashed) plotted with *condition subtraction* curves (solid) with increasing regadenoson doses towards the right with a 35-min wait time between injections.

To define the optimal regadenoson dose for BBB opening, each VSD fluorescence profile using different regadenoson doses (i.e., 100, 120, and 150 µl) was fit to an exponential of the

Biomedical Optics EXPRESS

form $\alpha + \beta e^{-\frac{t}{\tau_{diff}}}$. Figure 4(a) shows the raw VSD fluorescence profile obtained with a 150 µL regadenoson dose and 35 min wait time. The blue curve indicates the trace with VSD only and the red curve is with VSD + regadenoson administration. The dashed black vertical lines indicate the range of indices chosen for the proposed exponential curve fitting of the *condition subtraction* data in Fig. 4(b). It can be observed that the *injection curves* generally have 2-3 major peaks due to VSD recirculation, so the starting index was found by approximating the full-width-half-max (FWHM) of the first peak and multiplying it by four to account for approximately the end of the second peak. The last index was located about 15 sec after the *condition subtraction* curve reached a maximum value. To capture the differences in VSD perfusion with and without regadenoson administration, the diffusion time constant, τ_{diff}, corresponding to the time it takes for dye to diffuse into the tissue, was compared for different regadenoson doses (Fig. 3 shows the *condition subtraction* curves for each regadenoson dose with a 35 min wait time. The steepest slope appears in the case of 120 µL of regadenoson.). The steeper slope or smaller τ_{diff} implies greater BBB permeability due to faster diffusion and accumulation of the dye in the brain tissue. This contributes to a quicker increase in fluorescence intensity in the brain tissue region and thus a longer residence time and slower decay in terms of overall fluorescence intensity. The range of τ_{diff} for the *condition subtraction* curves was found by fixing α and β while varying τ_{diff} within a tolerance of 2 times the best fit's root-mean-square error (RMSE). Figure 4(b) shows the *condition subtraction* data in blue, the best fit as a solid green curve, and the τ_{diff} tolerance range which was from –3.40 sec to 3.36 sec presented as the dotted magenta and red curves, respectively.

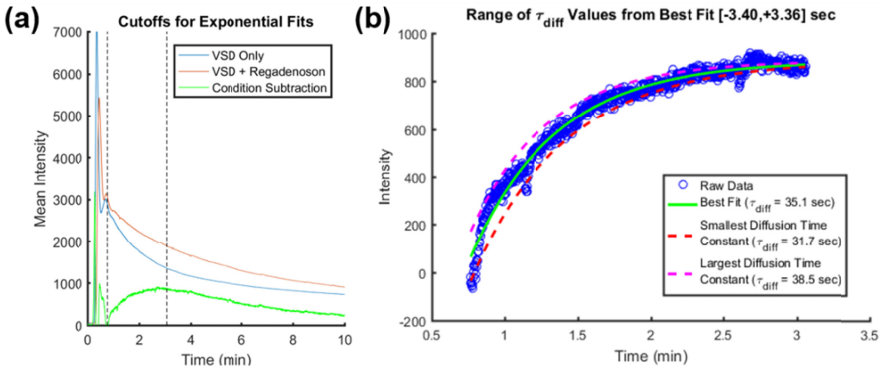

Fig. 4. Sample a) raw VSD fluorescence profiles with the selected range of *condition subtraction* curve indices for b) exponential fitting and analysis on the range of τ_{diff} values for fits within a tolerance of $2 \times RMSE_{BestFit}$.

The efficiency of different "wait times" between regadenoson and VSD injections was also evaluated. When comparing 5 or 20 min wait times to 35 or 55 min wait times (Fig. 5, left), the slope of the initial increase is much steeper in the latter cases. This is demonstrated by the diffusion time constants ($\tau_{diff,5min} = 29.5$ sec, $\tau_{diff,20min} = 39.2$ sec, $\tau_{diff,35min} = 15.9$ sec, $\tau_{diff,50min} = 5.7$ sec), which are inversely proportional to BBB permeability. The result suggests that regadenoson takes at least a few minutes to start having an effect on BBB permeability and the optimal wait time is 35 min or more.

Different doses of regadenoson were studied by changing the volume of regadenoson administered: 100, 120, and 150 µL at 5 and 35 min wait times (Fig. 5, right). To minimize

Biomedical Optics EXPRESS

side effects from different volumes, a constant total injection volume of 150 µL was maintained by filling any remaining volume with saline. As before, the slope of the *condition subtraction* curves was observed. The highest permeability and optimal dose appeared to occur when using 120 µL of regadenoson and 30 µL of saline. Interestingly, the wait time between regadenoson and VSD injections seems to have a diminished effect with increased regadenoson dose.

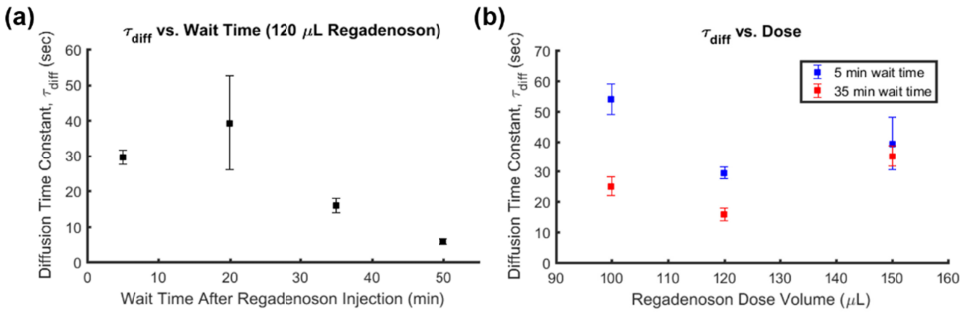

Fig. 5. Diffusion time constant (τ_{diff}) variation with a) wait time between injections and b) with regadenoson dose. Error bars represent the τ tolerance within $2\times RMSE_{BestFit}$.

A histological verification study was conducted to further support the findings. Three rats were injected with regadenoson only, both regadenoson and VSD, and VSD only, respectively. Figure 6 shows the small signal for the first rat, where only a low-level autofluorescence background can be observed. The brain slices of the third rat show substantial VSD fluorescence, but this signal is markedly less compared to the second rat with VSD + regadenoson. This confirms regadenoson's potential as a VSD delivery agent, indicating its ability to increase VSD concentration in superficial and deep brain tissue layers through the BBB to facilitate increased-depth brain imaging.

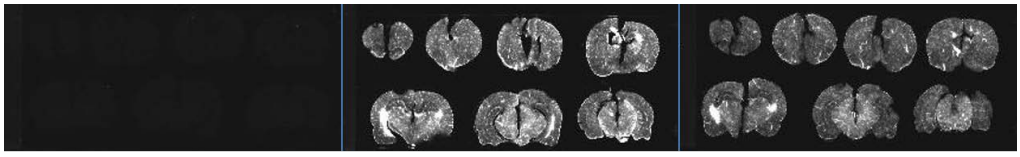

Fig. 6. Brain slices with regadenoson only (left), regadenoson + VSD (middle), and VSD only (right).

Discussion and conclusion

We have presented the effectiveness of adenosine receptor agonist, regadenoson, in increasing the BBB permeability to allow greater VSD diffusion into the brain tissue for brain activity monitoring applications at increased imaging depths. We have shown that a regadenoson dose volume of about 120 µL with a wait time of at least 35 min increases the BBB permeability the most.

In our first through-skull fluorescence imaging validation studies with intact skulls, the lack of stereotaxic fixation increased noise in our signal. The sudden variations of the signal seen in Fig. 2(a) are likely due to mouse movements as anesthesia wore off and from breathing. Even if the mice did not move their heads outside the ROI, the fluorescence signal changed due to the beam not being perfectly uniform in intensity and the fluorescence signal intensity's dependence on the incident intensity. To control for these movement-induced changes, all the following studies included stereotaxic fixation. However, this stabilized the skull, which minimized movement, but still large brain pulsing and sudden involuntary movements within the ROI could create small variations in the signal as in Fig. 3(a).

Biomedical Optics EXPRESS

Additionally, although the same amount of VSD was injected for each mouse, variability can be observed in the peak intensities of the *injection curves*. These differences in the fluorescence signal are likely due to anatomical differences from mouse to mouse in addition to the position of the mouse brains under the non-uniform beam as discussed above.

After the first studies, in which the VSD fluorescence was monitored for 1 hour after each dye injection, it was found that the fluorescence intensity reached a steady state before 30 minutes. In order to keep the mouse anatomy constant, the same mouse was used for both conditions (VSD only and VSD + regadenoson). To account for remaining fluorescence after any previous VSD injections, a background image was taken before each 30 min monitoring session when it was assumed that any further decay in fluorescence signal due to previous injections was negligible. This background image was subtracted from images collected from the proceeding VSD injection.

For the optimization of regadenoson dose and timing studies, the cranial windows varied slightly in their locations for each mouse. However, roughly equivalent ROIs were chosen based on in-focus major vasculature versus out-of-focus microvasculatures. It can also be seen in the results (Fig. 3) that all the ROIs have approximately the same time course trend but varied slightly in their intensities. Equivalent ROIs were also used to measure diffusion time constants through exponential curve fitting.

regadenoson is routinely used for cardiac stress testing, raising a concern about how faster heart rate and circulation affects the results. However, with increased circulation, it would be reasonable to expect faster flushing out of the VSD from the circulatory system. Astellas, the manufacturer of regadenoson, also warns of changing blood pressure (increase or decrease), which could contribute to the difference in slopes of the *condition subtraction* curves.

Another concern is with regard to dosage based on weight. Clinically, regadenoson is given to humans at the same concentration and volume regardless of weight or size. Thus, in this study, the same concentration and volume were given regardless of animal weight or size, mimicking the human protocol. We approximated the mouse dose based on the clinical human dose and the ratio between average mouse and human weights. We found this dose was insufficient, possibly due to the higher metabolism, heart rate, etc. of mice as compared to humans. The rat dosage used for histopathological studies that was effective in increasing BBB permeability was similar to that used in the mice, although the rats weighed significantly more and their metabolism is much slower than that of mice. Alternatively, anesthesia may have cardiac implications, which could alter regadenoson's dilatory effects. Perhaps rodent dose can be generalized, but for animals with weights more than an order of magnitude different, slight adjustments may need to be made for the optimal conditions.

Overall, this study validated the use of venous injections of regadenoson for BBB opening to deliver NIR VSD, IR-780 perchlorate. It also demonstrated the possibility of using IR-780 VSD for minimally invasive through-skull fluorescence imaging of neuronal activity. General dosage and timing guidelines were created for optimal VSD diffusion results.

Funding

National Institute of Health (NIH) (MH106083); National Science Foundation (NSF) (MRI1430040).

Disclosures

The authors declare there are no conflicts of interest related to this article.